Available online at www.sciencedirect.com
ScienceDirect
Journal of Pharmaceutical and Biomedical Analysis 45 (2007) 251–256
JOURNAL OF PHARMACEUTICAL AND BIOMEDICAL ANALYSIS
www.elsevier.com/locate/jpba

A simple model for complex dissolution kinetics: A case study of norfloxacin

Peter J. Skrdla *

640 Maple Street, Westfield, NJ 07090, USA

Received 25 April 2007; received in revised form 8 June 2007; accepted 11 June 2007
Available online 15 June 2007

Abstract

A new semi-empirical model, particularly useful for studying complex dissolution kinetics, is presented here. It uses only two 'fit parameters', each possessing physically relevant units (in the time domain). The model is based on the idea that dispersion (variation) in the activation energy barrier may arise in certain cases, as a result of (quantized) molecular kinetic energies affecting the speed of the rate-determining step (r.d.s.) of the dissolution event. For such 'dispersive dissolutions', the r.d.s. is assumed to involve 2D denucleation. The author's dispersive kinetic model is shown to be applicable to the dissolution of various formulations of norfloxacin which produce very asymmetric, sigmoidal concentration versus time (*C–t*) profiles. It is derived by assuming an activation energy distribution having the functional form of the Maxwell–Boltzmann (M–B) distribution, coupled with a first-order rate expression. However, this model can also be reduced to give the same functional form as the classical Noyes–Whitney equation, in order to accurately fit/describe dissolution profiles which appear logarithmic (such profiles are due to dissolution phenomena that are not dispersive; i.e. for cases where the activation energy is essentially single-valued). Thus, the kinetic model presented in this work may potentially find broad applicability to the modeling of various dissolution trends observed in the literature.

Keywords: Dissolution; Dispersive kinetics; Model; Norfloxacin; Sigmoid; Maxwell–Boltzmann

1. Introduction

Dissolution research has grown in importance in the pharmaceutical sciences over the last century, mainly due to the increased awareness of the community of the fact that the dissolution properties of drug products can often help predict their bioavailability. However, dissolution research is also important in other fields, including geology and cosmology, e.g. [1]. Unfortunately, the 'universal modeling' of dissolution kinetics using a mathematically simple equation, and, thus, an accurate explanation for all types of dissolution behavior (i.e. various concentration versus time, *C–t*, curve shapes), has remained largely out of reach. Beyond the simple, first-order, Noyes–Whitney equation and the highly specific, mathematically complex, numerical methods of present-day (which are based mainly on Fick's laws of diffusion and various *macroscopic* properties of the solids under investigation), the fundamental mechanism(s) of dissolution is/are not completely understood.

This work presents a novel 'dispersive kinetic' model for dissolution processes, which the author believes may be very general (perhaps universal) in application. That is because the model introduces a fundamental, *microscopic* property of all converting (i.e. reacting/transforming) systems: quantized, molecular kinetic energies. Although the development of this model has been described in previous works and its application to modeling various 'homogeneous dispersive' solid-state conversions, i.e. those producing deceleratory, sigmoidal *C–t* curves, has been discussed (as will be described later in Section 2), this work represents the author's initial attempt at using the model to study dissolution phenomena. The author has selected to try to apply the model to the dissolution of various norfloxacin formulations in this work, because of the challenging curve shapes produced by this compound.

1.1. Background

A recent review of the dissolution literature has been published [2], providing a historical perspective of dissolution modeling from the Noyes–Whitney equation to present-day

* Tel.: +1 908 232 0572.
E-mail address: skrdla@earthlink.net.

0731-7085/$ – see front matter © 2007 Elsevier B.V. All rights reserved.
doi:10.1016/j.jpba.2007.06.012

numerical methods, e.g. [3]. Additionally, Dokoumetzidis and co-workers discuss in their review the development and use of the Biopharmaceutics Classification System (BCS), as a basis for establishing relationships between dissolution and bioavailability. The reader is referred to this work for additional details regarding current dissolution technology and practices.

The isothermal Noyes–Whitney equation, originally published in 1897, relates the rate of dissolution of solids to the macroscopic properties of the solid and the dissolution medium. In 1904, Nernst and Brunner modified this equation by applying Fick's First Law of Diffusion to establish a relationship between the dissolution rate and the diffusion coefficient. The Nernst–Brunner equation may be written as

$$\frac{dC}{dt} = \left(\frac{DA}{LV}\right)(C_s - C) \quad (1)$$

where dC/dt is the rate of dissolution of the compound (typically, the active pharmaceutical ingredient, API), D the diffusion coefficient of the molecule, L the diffusion layer thickness, A the surface area of the solid, V the volume of the dissolution medium (which is stirred rapidly to ensure homogeneity), C the concentration of the dissolved solid in the dissolution medium and C_s is the concentration of the dissolved solid in the diffusion layer surrounding the solid. Despite the maturity of Eq. (1), this dissolution model remains widely used in present-day pharmaceutical research.

Upon further inspection, it is clear that Eq. (1) is reducible to a simple, first-order (i.e. F1) kinetic model. The integrated version of Eq. (1) may be written as

$$\frac{C}{C_\infty} = 1 - \exp(-kt) \quad (2)$$

where C_∞ is the dissolved concentration as $t \rightarrow \infty$ and k is the rate constant (i.e. as defined by the classical Arrhenius equation). Note that k has units of $(\text{time})^{-1}$ for a first-order rate law; also, k incorporates into it the term 'DAC_s/LV' of Eq. (1). This first-order model for dissolution adequately explains logarithmically increasing 'conversion–time' (C–t, or C/C_∞–t) kinetic profiles.

While many dissolution curves obey Eq. (1)/Eq. (2), a general dissolution mechanism has not been fully elucidated to this day, e.g. [4]. The most challenging feature of common C/C_∞–t dissolution curves is their asymmetric, sigmoidal shape, which is not properly explained by these equations. This sigmoidal behavior has been (qualitatively) attributed to various macroscopic events, e.g. [5]: 'mechanical lag' and 'wetting' are believed to define the initial 'induction period', while both 'disaggregation' and 'disintegration' are thought to contribute to the actual dissolution process, which follows the induction period. Because it is poorly understood and difficult to model, some workers may select not to model the induction period in their kinetic treatments.

Some of the most significant contributions to the dissolution kinetics literature, beyond Eq. (1), include the models proposed by Higuchi [6] and Peppas [7]. These '1D Diffusion' and 'Power Law' models have proven their effectiveness in a wide range of drug release studies. It should be noted that these models are also commonly employed in the thermal analysis literature [8–10]. Additionally, they may find origin in the field of dispersive kinetics [11,12], which will be discussed later. The general functional form of these models is given by

$$\frac{C}{C_\infty} = kt^n \quad (3)$$

where n is a parameter whose value can be obtained from curve-fitting of the C/C_∞–t kinetic data. A key drawback of the models based on Eq. (3) is that n is often empirical; i.e. it has a value which does not satisfy any particular model that has been mathematically derived to-date, e.g. [9]. Nonetheless, Burch and coworkers have utilized parallel (simultaneous) empirical 'Power Law' rate equations to model the dissolution kinetics of albite [13].

The so-called 'Weibull function' has a mathematical form which appears to combine Eqs. (2) and (3):

$$\frac{C}{C_\infty} = 1 - \exp(-kt^n) \quad (4)$$

Eq. (4) has been utilized in several works to describe dissolution and drug release kinetics, e.g. [14,15]. However, the use of this model has received criticism because it also employs the 'non-physical' (i.e. empirical) fit parameter, n. On the other hand, Eq. (4), with $n = 2$, 3 or 4, are often referred to (collectively) as the Avrami–Erofe'ev (A2–A4) models in the thermal analysis literature, e.g. [8–10]. Eq. (4) may also be called the Johnson–Mehl–Avrami (JMA) model, for instance when it is applied to the crystallizations of pharmaceutical compounds, e.g. [16]. From the dispersive kinetics literature, it has recently been found that the equation can be obtained from the Kohlrausch–Williams–Watts (KWW) relaxation function or 'stretched exponential', utilizing the concept of 'fractal time' [11,12]. However, as Eq. (4) was mathematically derived and first applied to solid-state conversions more than 60 years ago, e.g. see Refs. [17,18], its relatively recent introduction to dissolution research literature may be somewhat surprising.

Recent numerical methods have utilized macroscopic properties such as particle size distributions and fragmentation functions to describe dissolution, e.g. [3]. Unfortunately, many of these approaches require the solution of simultaneous differential equations, which may not be feasible in many analytical laboratories [2]. Additionally, the use of macroscopic parameters (which may also include a particle 'shape factor', e.g. [3]) may make these models highly specific. Thus, a simple yet general dissolution model which can be applied to a wide range of crystal morphologies, particle sizes, etc., to be used predominantly for describing/fitting highly asymmetric, sigmoidal C/C_∞–t curves, may be very desirable. The author puts forth the present work mindful of this goal.

2. Results and discussion

The author believes that the observation of asymmetric, sigmoidal dissolution profiles, like many other phase transitions and chemical reactions involving the solid-state, may be due to 'dispersion' (variation) in the activation energy/rate constant of 'classical kinetic' (e.g. first-order) processes. Classical kinetics

inherently defines a single activation energy and, hence, a single rate constant (i.e. following the theories of Arrhenius or Eyring) for each step of a given conversion. On the other hand, dispersive kinetics are typically observed in conversions for which the rate of 'system renewal' (e.g. relaxation), is comparable to, or slower than, the rate of the conversion [11,12]—in this case, dissolution. The result of this dispersion is a distribution of activation energies. If one assumes that this activation energy distribution takes the functional form of the Maxwell–Boltzmann (M–B) kinetic energy distribution, it is possible, using Eq. (2), to derive (using a mathematical approximation for purposes of simplification [10]) the model equation shown below, as described elsewhere [17,18]:

$$\frac{C}{C_\infty} = 1 - \exp\{[\alpha t][\exp(-\beta t^2) - 1]\} \quad (5)$$

In Eq. (5), α and β are kinetic parameters with units of $(\text{time})^{-1}$ and $(\text{time})^{-2}$, respectively, which makes them akin to more traditional (global) rate constants. The fact that Eq. (5) contains only two 'fit parameters', each with physically meaningful units, helps make it a semi-empirical kinetic model (compared to Eqs. (3) and (4), which are most often applied empirically). Note that in the derivation of Eq. (5), a dimensionality of two was assumed based on current knowledge of the mechanisms involved in crystal growth and Ostwald ripening, e.g. see [18]. The author believes that the process of '2D denucleation', particularly with small critical nuclei, may be involved in the rate-determining step (r.d.s.) of many dispersive dissolution processes (i.e. those which produce deceleratory, sigmoidal C/C_∞–t profiles); it is the molecular kinetic energies pertaining to this r.d.s. that are quantized in the author's model, as discussed previously [17,18]. However, based on experience [16], Eq. (5) may also be used to describe more logarithmic C/C_∞–t profiles, for cases where dispersion is not observed experimentally. That is because if dispersion in the activation energy/rate constant does not affect the dissolution rate, the overall rate constant for the process, $k(t)$ (which is defined as $k(t) = \alpha' \exp(-\beta t^2)$ for various homogeneous dispersive conversions in the author's previous works [17,18]), becomes time-independent (because $\beta = 0$) and hence single-valued, as per the Arrhenius/Eyring definitions. For such cases, $k(t) = \alpha'$, a constant (*note*: the 'primed' symbol serves only to differentiate it from α in Eq. (5)), essentially reducing Eq. (5) to Eq. (2).

The sigmoidal C/C_∞–t dissolution curves collected by Dos Santos et al. [19] for various formulations of the API, norfloxacin, are investigated in this work. This data was selected because the dissolution curves of norfloxacin exhibit pronounced induction periods as well as distinct asymmetry. These features make them difficult to characterize accurately/precisely using the general dissolution models discussed in Section 1.1. The sigmoidal behavior, alone, makes these curves difficult to describe using Eq. (2). While Eq. (4) is often successful (in the author's experience) at modeling symmetrical C/C_∞–t sigmoids, it has difficulty describing more asymmetric trends and, furthermore, it does not define a precise start time for the conversion (thus, it does a poor job of explaining the induction period, e.g. [20]). Papadopoulou et al. have noted in a recent work that values of n in Eq. (4) that are greater than unity generally correspond to sigmoid curves which may be 'indicative of complex release mechanisms' [14].

As an aside, the type of experimental apparatus used by Dos Santos et al. [19], which inevitably introduces a 'time lag' between the solution sampling and analysis, is not thought to dramatically affect the dissolution profiles shown in this work because the lag can be considered to be essentially constant over the course of the experiment (perhaps, with some *random* variation); thus, it cannot be responsible for the slower initial rate observed at the start of the experiment (the induction period) relative to that at the mid-point of the dissolution event, i.e. the sigmoidal C/C_∞–t trends in which the (specific) dissolution rate changes *systematically* over the course of the conversion. For this reason, the dissolution profiles of various APIs/their formulations collected using such (traditional) equipment are thought to accurately reflect the kinetics of the r.d.s. of the overall mechanism, and are not expected to be significantly affected by experimental artifacts.

In contrast to Eq. (2), Eqs. (3)–(5) can be seen (by examining Figs. 1 and 2 and Table 1) to describe the complex dissolution profiles of norfloxacin reasonably well. Furthermore, this equation defines the start time of dissolution at exactly $t = 0$. The author believes that Eq. (5) may be the simplest kinetic model in the literature that most accurately explains all types of dissolution data. As this model attributes the (asymmetric) sigmoidal shapes exhibited by many dissolution curves to molecular-level dispersion in the activation energy barrier (which ultimately gives rise to the existence of the 'M–B-like' distribution of activation energies mentioned earlier), it represents a very different view of dissolution kinetics from the macroscopic models most often presented in the literature, to-date.

The quality of the regression fits to the dissolution profiles in Fig. 1, using Eq. (5), can be seen to range from $R^2 = 0.983$

Table 1
Kinetic parameters extracted from the data points in Fig. 1 using regression fits of Eq. (5) (see text for details). In parentheses are shown the corresponding standard errors

Formulation	Fit quality, R^2	α (min)	β $(\text{min})^{-2}$	Standard error of estimate
Norfloxacin/Na caprate 1:5	0.994	30 (900)	3×10^{-4} (1×10^{-2})	0.0316
Norfloxacin/Na caprate 1:1	0.982	30 (1000)	3×10^{-4} (1×10^{-2})	0.0557
Norfloxacin/EDTA 1:5	0.998	20 (200)	2×10^{-4} (2×10^{-3})	0.0210
Norfloxacin/EDTA 1:1	0.998	7.04×10^{-2} (1.1×10^{-3})	1.45×10^{-2} (8×10^{-4})	0.0160
Norfloxacin	0.996	9.88×10^{-3} (9×10^{-5})	1.1×10^{-1} (8×10^{-2})	0.0092

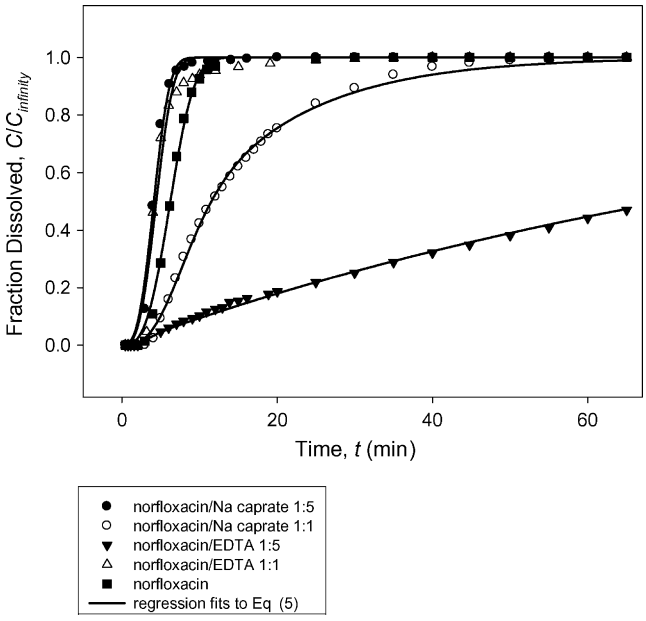

Fig. 1. Dissolution profiles for various norfloxacin formulations, extracted from Ref. [19]. The lines represent regression fits of the data using Eq. (5); see Table 1 for details.

to 0.998. Overall, the good quality of these fits supports the use of the model in the kinetic modeling of dispersive dissolution curves and it helps to verify some of the initial assumptions made during the development of the equation [10,17,18]. Note that Eq. (5) has been used previously by the author to fit the kinetic data of other homogeneous dispersive processes (i.e. conversions which also produce deceleratory C/C_{∞}–t sigmoids), including the thermal decomposition of various crystalline compounds [10,17,18].

The values of the α and β parameters extracted from these regression fits (see Table 1), when used together in Eq. (5), may be used to obtain a reasonable prediction of the dissolution time required to achieve a desired solution concentration, for each of the norfloxacin formulations presented in this work (at constant temperature). Note, however, that as the rate of dissolution is dependent on both the relative magnitudes of α and β as well as the absolute value of each parameter, a direct comparison of the dissolution rates using the values in Table 1 can be somewhat challenging. This issue is further compounded by the large errors associated with some of the rate parameters in the table; only for two of the five formulations are the standard errors for α and β smaller than their determined values. However, despite this finding, the standard errors of estimate of the regression fits appear to be quite reasonable. For example, for the slowest-dissolving norfloxacin/EDTA 1:5 formulation, after 65 min of dissolution time, the difference between the actual (experimentally determined) amount of drug dissolved and the amount predicted from Eq. (5) is −0.9%. For comparison, for the fastest-dissolving norfloxacin/Na caprate 1:5 formulation, the corresponding difference (after 65 min) is 0.0%.

Fig. 2 serves largely to exemplify the observation that it may be possible to obtain reasonably good fits to essentially all of the data points, even for 'complex dissolution curves', using Eq. (5). For this reason, the practice of disregarding the induction period in the modeling of dissolution kinetics should be discouraged, particularly because the induction period is a key component of many dissolution profiles and because Eq. (5) provides a general, physical explanation for its existence (i.e. beyond the previously reported, qualitative observations mentioned in Section 1.1) which further supports its use in kinetic modeling; the duration of the induction period is established largely by the

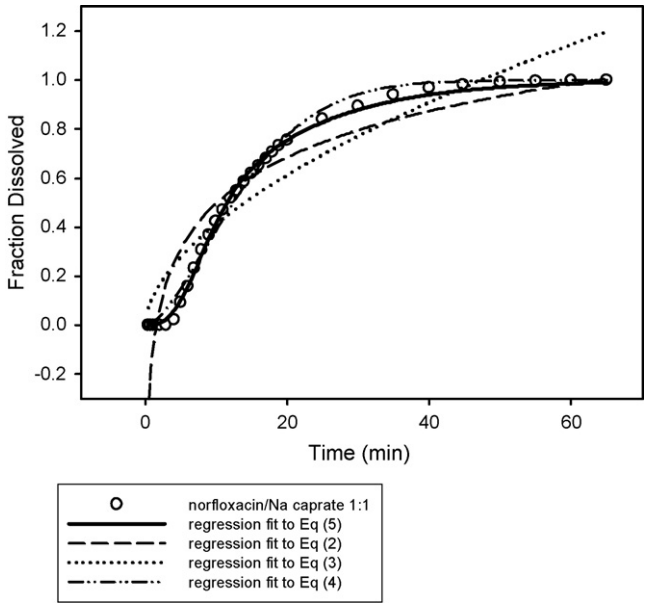

Fig. 2. Dissolution profile for the norfloxacin/EDTA 1:1 formulation in Fig. 1, presented alone for improved clarity. The thick, solid line represents a regression fit of the data using Eq. (5); $R^2 = 0.998$. The other lines are regression fits to the same data using the conventional kinetic models described in the text; fit quality varies from $R^2 = 0.893$ for Eq. (2) to $R^2 = 0.993$ for Eq. (4).

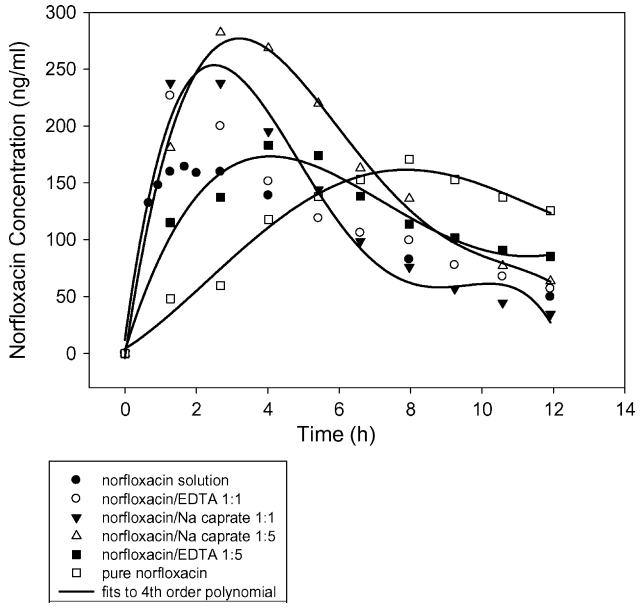

Fig. 3. Mean plasma concentration of norfloxacin vs. time (0–12 h) profiles obtained following oral dosing of rabbits at 10 mg/kg using various drug preparations, reproduced from Ref. [19]. The lines represent regression fits of the data points to a fourth-order polynomial, for four of the six formulations; see Table 2 for details.

Table 2
Coefficients extracted using regression fits of the equation $y = a + bx + cx^2 + dx^3 + ex^4$ (i.e. for a 'y vs. x' plot) to the data points in Fig. 3. See text for details

Formulation	Fit quality, R^2	a	b	c	d	e
Norfloxacin/Na caprate 1:5	0.994	−3.375	213.0	−52.40	4.572	−0.1372
Norfloxacin/Na caprate 1:1	0.968	12.10	231.0	−70.56	7.361	−0.2566
Norfloxacin/EDTA 1:5	0.962	2.613	101.3	−19.32	1.268	−0.0260
Norfloxacin	0.978	4.299	19.19	4.557	−0.7982	0.0295

relative magnitudes of the rate parameters, α and β, in Eq. (5). On the other hand, for cases of very slow dissolution, the latter part of the dissolution curve may be of more interest to workers than the initial portion. Note that the regression fits of the other models presented in Section 1 to the dissolution curve in Fig. 2 are not as good as the fit of Eq. (5).

To present a possible area for future work, the bioavailability data from Ref. [19] is also reproduced here, in Fig. 3 (see figure caption for experimental details). In this figure, the data points were *arbitrarily* fit to a fourth-order polynomial using regression analysis. Four of the six 'fit curves' generated were found to be visually reasonable in modeling the data: these curves correspond to the pure norfloxacin, norfloxacin/EDTA 1:5, norfloxacin/Na caprate 1:1 and norfloxacin/Na caprate 1:5 formulations. The fits of the data sets for each of these four formulations are shown in the figure and the corresponding regression fit parameters are provided in Table 2. The quality of the fits was found to range from $R^2 = 0.962$ to 0.994. For the remaining two data sets, the larger degree of scatter in the data points (mainly at longer t) produced what appeared to be bimodal dissolution behavior; thus, these fit curves were omitted from the figure and they are also not described in the table.

Mathematical integration of the fit functions described in Table 2 yielded corresponding 'area-under-curve' (AUC) exposures, as a function of time (i.e. following administration). These 'AUC_{0-t}' functions (one for each of the four formulations fit in Fig. 3) are plotted in Fig. 4. As these plots also appear sigmoidal, it is possible that the net/cumulative exposure of the various oral formulations of norfloxacin may be represented by a mathematical convolution of the dissolution profiles (i.e. the curves in Fig. 1) with some 'biological action' function(s). The implication of this observation is clear: if one can accurately/consistently model dissolution profiles in the laboratory (i.e. with Eq. (5), or its simplified form, Eq. (2), depending on whether or not the dissolution is dispersive), it may, resultantly, be possible to differentiate (i.e. 'subtract out') a drug's native dissolution kinetics from the *in vivo* contribution responsible for producing the overall exposure for a particular compound and/or formulation. Thus, it may ultimately be possible to extract (global) '*in vivo* functions' from the AUC data (for which models can then be developed in the future) which describe the kinetics of the bodily functions relevant to the given exposure profile.

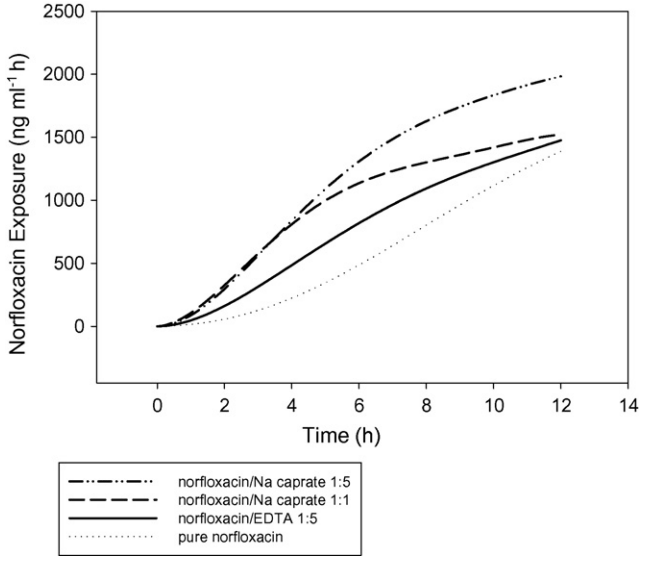

Fig. 4. Plots of the integrated fit functions shown in Fig. 3 (i.e. for the four formulations listed in Table 2), yielding corresponding norfloxacin exposures (AUC_{0-t}) as a function of time.

3. Conclusions

Eq. (5), which is presented here as a novel, dispersive kinetic model for dissolution, is based on the assumptions of an activation energy distribution of the Maxwell–Boltzmann type, a first-order kinetic rate law and a '2D denucleation' rate-limiting step. The model was shown to accurately describe the complex dissolution profiles of various formulations of norfloxacin. As the equation has the ability to fit both sigmoidal (dispersive) and logarithmic (non-dispersive, i.e. first-order or 'Noyes–Whitney/Nernst–Brunner-like') C/C_∞–t trends, it is believed that Eq. (5) may potentially serve as a simple yet universal model for dissolution.

References

[1] R. Hellmann, D. Tisserand, Geochim. Cosmochim. Acta 70 (2006) 364–383.
[2] A. Dokoumetzidis, P. Macheras, Int. J. Pharm. 321 (2006) 1–11.
[3] D. Mangin, E. Garcia, S. Gerard, C. Hoff, J.P. Klein, S. Veesler, J. Cryst. Growth 286 (2006) 121–125.
[4] M. Blanco, M. Alcala, J.M. Gonzalez, E. Torras, Process Anal. Technol. 3/5 (2006) 25–29.
[5] A.R. Gennaro (Ed.), Remington: The Science and Practice of Pharmacy, 20th ed., Lippincott Williams & Wilkins, Baltimore, 2000.
[6] T. Higuchi, J. Pharm. Sci. 50 (1961) 874–875.
[7] N.A. Peppas, Pharm. Acta Helv. 60 (1985) 110–111.
[8] A. Khawam, D.R. Flanagan, J. Pharm. Sci. 95 (2006) 472–498.
[9] A. Khawam, D.R. Flanagan, J. Phys. Chem. B 110 (2006) 17315–17328.
[10] P.J. Skrdla, R.T. Robertson, Thermochim. Acta 453 (2007) 14–20.
[11] A. Plonka, Sci. Rev. 25 (2000) 109–218.
[12] A. Plonka, Annu. Rep. Prog. Chem. C 97 (2001) 91–147.

[13] T.E. Burch, K.L. Nagy, A.C. Lasaga, Chem. Geol. 105 (1993) 137–162.
[14] V. Papadopoulou, K. Kosmidis, M. Vlachou, P. Macheras, Int. J. Pharm. 309 (2006) 44–50.
[15] K. Kosmidis, P. Argyrakis, P. Macheras, Pharm. Res. 20 (2003) 988–995.
[16] P.J. Skrdla, J. Pharm. Sci. 96 (2007) 2107–2110.
[17] P.J. Skrdla, R.T. Robertson, J. Phys. Chem. B 109 (2005) 10611–10619.
[18] P.J. Skrdla, J. Phys. Chem. A 110 (2006) 11494–11500.
[19] I. Dos Santos, F. Fawaz, A.M. Lagueny, F. Bonini, Int. J. Pharm. 260 (2003) 1–4.
[20] P.J. Skrdla, J. Phys. Chem. A 108 (2004) 6709–6712.